The Media Calibration System for Cassini Radio Science: Part I

C. Naudet,[1] C. Jacobs,[1] S. Keihm,[2] G. Lanyi,[1] R. Linfield,[3] G. Resch,[1] L. Riley,[2]
H. Rosenberger,[2] and A. Tanner[2]

Accurate calibration of line-of-sight delay fluctuations in the Earth's atmosphere will be essential for future radio science experiments. In particular, the sensitivity of the Cassini gravitational wave experiment (GWE) will be limited by the performance of the calibration system of water-vapor-induced path delay. We have designed and built a high-accuracy troposphere calibration system. The primary components of this system are a pair of narrow-beam, gain-stabilized water vapor radiometers.

From September 1999 to May 2000, we conducted tests at Goldstone, comparing the path delays produced by our calibration system with the line-of-sight delays measured with a radio interferometer at 8.4 GHz on a 21-km baseline. Application of our troposphere calibration measurements reduced the Allan standard deviation of the delay fluctuations on all time scales >20 s. On time scales >1000 s, the performance is within a factor of 2 of the GWE requirements. The limiting errors in this comparison appear to lie with the radio interferometry (instrument stability and geometrical modeling). Therefore, we expect further improvement with additional analysis. This article, Part I, reports on the results of the series of performance-testing experiments conducted at Goldstone from September 1999 to May 2000. A future article, Part II, will discuss the details of the instrumentation, observing strategy, data analysis procedures, and error budget.

I. Introduction

Over the last several years, we have been developing an atmospheric media calibration system in support of the Cassini radio science experiments. The Cassini spacecraft was launched in 1997, will arrive at Saturn in 2004, and will start radio science experiments during its cruise phase (early 2001). The Cassini gravitational wave experiment (GWE) has been described in detail by Armstrong and Sramek [1] and Tinto and Armstrong [2]. Detailed studies of the GWE error budget [3,4] point to atmospheric delay fluctuations as the dominate error component on time scales greater than 100 s. Thus, the sensitivity

[1] Tracking Systems and Applications Section.

[2] Microwave and Lidar Technology Section.

[3] Infrared Processing and Analysis Center, California Institute of Technology, Pasadena.

The research described in this publication was carried out by the Jet Propulsion Laboratory, California Institute of Technology, under a contract with the National Aeronautics and Space Administration.

of the GWE will be limited by the ability to calibrate out these atmospheric delay fluctuations. Since almost all the power in the atmospheric delay fluctuations at frequencies less than 0.01 Hz is due to the wet troposphere, the principal instrumentation used for calibration is a water vapor radiometer.

An advanced water vapor radiometer (WVR), shown in Fig. 1, was developed at JPL and is described in detail by Tanner [5]. The WVR has an off-axis reflector, giving a 1-deg beam width with very low side lobes. The pointing accuracy is 0.1 deg. The WVR measures the brightness temperature at 22.2, 23.8, and 31.4 GHz, with long-term stability of 10 mK on time scales of ∼10,000 s. The path delay along the line of sight depends on the integrated columnar density of water vapor and may be estimated by measuring the strength of the 22.2-GHz spectral line of water. In order to reduce the sensitivity to variable height distribution of the water vapor, and to the presence of clouds, we use two additional frequency channels at 23.8 and 31.4 GHz [13]. The WVR acquires data in subsecond intervals and produces a time series of line-of-sight brightness temperatures. Off to the right in the background of the picture, one can see the microwave temperature profiler (MTP). The MTP retrieves the vertical distribution of atmospheric temperature. The data from the WVR, MTP, and surface meteorological stations are then post-processed with two retrieval algorithms [8,9] to extract the line-of-sight delay. This article, Part I, will report on the results of the series of performance-testing experiments conducted at Goldstone from September 1999 to May 2000. A future article, Part II, will discuss the details of the instrumentation, observing strategy, data analysis procedures, and error budget.

II. Performance Testing

The objective of the atmospheric media calibration system is to measure the atmospheric path-delay fluctuation of signals transmitted between the Cassini spacecraft and the Goldstone DSS-25 antenna. Two advanced WVRs have been built to support Cassini radio science experiments. Dual WVRs allow

Fig. 1. The media calibration subsystem at DSS 13 in Goldstone, CA. The new advanced WVR is seen in the center, and the MTP is shown in the background to the right.

for operational reliability and robustness in the case of equipment failure and for cross-checks between the units. A detailed comparison of the two units has been made [5], and the Allan standard deviation [10] was shown to be significantly better than the GWE requirements for all interval times greater than 100 s. However, this side-by-side comparison reflects only the stability of the WVR. In order to demonstrate the accuracy of a WVR, it is necessary to compare one with results from another measurement technique. Following earlier successful comparison experiments utilizing older-model WVRs [6,7], a connected-element interferometer (CEI) was used to independently measure the line-of-sight path-delay fluctuations. An overview of the experimental setup is shown in Fig. 2.

From August 1999 until May 2000, we conducted a series of dual-frequency (2.3- and 8.4-GHz) CEI observations on the 21-km baseline between the Deep Space Network (DSN) high-efficiency 34-m-diameter antenna at DSS 15 and a 34-m-diameter beam-waveguide antenna at DSS 13. Since the effective wind speed is typically less than 5 to 10 m/s, the tropospheric fluctuations at each site will be independent for time scales less than ∼4000 s, making this baseline well-suited for a WVR comparison experiment. Strong, point-like radio quasar sources (flux density > 1 Jy) with accurately known positions were chosen to minimize CEI errors. The data from each antenna were cross-correlated, and the interferometric delay (the difference in arrival times at the two antennas) was extracted. After subtraction of an a priori model, the residual phase delay (phase divided by the observing frequency) and delay rate (the time rate of change of the phase delay) were obtained. In addition, a linear clock model was fitted to the data [11] and removed.

Each WVR was positioned ∼50 m from the base of the 34-m antenna. This offset was chosen to maximize the sky coverage while minimizing the magnitude of beam-offset errors [12].[4] The WVR was

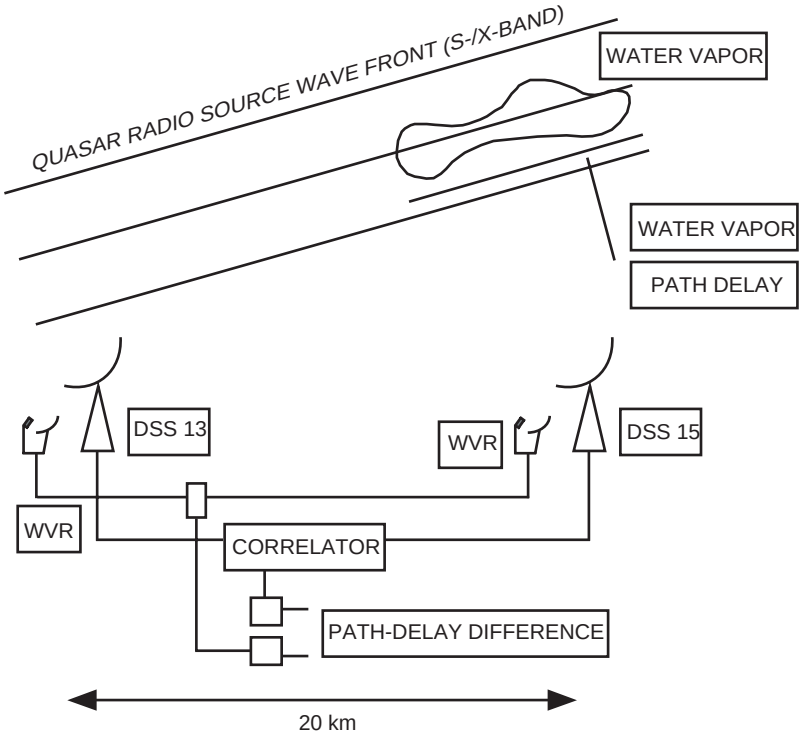

Fig. 2. A schematic representation of the WVR–CEI comparison experiments.

[4] R. P. Linfield, "Error Budget for WVR-Based Tropospheric Calibration System," JPL Interoffice Memorandum 335.1-96-012 (internal document), Jet Propulsion Laboratory, Pasadena, California, June 5, 1996.

co-pointed with the DSN antennas during sidereal tracking of distant natural radio sources. The WVRs were monitored in real time, and derived path-delay time series were produced during post-processing at JPL. After the WVR path-delay time series were smoothed over 6 s, the WVR data from each site (DSS 15 and DSS 13) were subtracted to create a site-differenced delay time series. Finally, the data were fitted for clock-like effects, resulting in a differenced WVR data type that could be directly compared with the CEI residual phase delays.

The comparison experiments conducted in 1999 were limited in scan duration to less than 26 min (the duration of a single pass on the CEI tape recorder). Several experiments produced little data, due to an assortment of instrumental problems and operator errors. In addition, instrumental problems at DSS 13 caused uncalibrated delay errors on long (>1000 s) time scales. A fairly representative experiment is DOY 240, 1999. This experiment consisted of 11 scans, each of ∼26-min duration, covering a wide variety of azimuths and elevations. For ease of comparison between data sets at different elevations, both the CEI and WVR data sets have been converted (mapped) to the equivalent delays in the zenith direction.

A time series of the site-differenced residual phase delay for both the CEI and WVR data for scan 3 is shown in Fig. 3. It is clear that the correlation between the two data sets is strong. The CEI data can be corrected for phase-delay fluctuations by subtracting the corresponding WVR data. Figure 4 shows the time series of the WVR-corrected CEI data (calibrated CEI data). The rms of the calibrated CEI is 0.5 mm, a factor of 3 improvement from the initial 1.7 mm. The distribution of the CEI residuals before and after WVR correction for all scans on DOY 240, 1999, is shown in Fig. 5. The site-differenced residual-delay rms is seen to change from ∼1.1 mm before WVR calibration to ∼0.4 mm after calibration.

By May 2000, we were able to correct long-term CEI instrumental stability problems, enabling WVR–CEI comparison over very long time scales (>1000 s). Two experiments, on DOY 137, 2000, and DOY 138, 2000, were conducted after these long-term stability problems were corrected. The CEI and WVR delay time-series data from DOY 138, 2000, are shown in Fig. 6. The CEI and WVR residual path-delay data sets track closely. The CEI data have an rms of ∼4.3 mm. After WVR calibration, this is reduced to ∼1 mm, a factor of 4 improvement. On DOY 137, 2000, an improvement factor of 1.7 was measured; however, the surface winds were measured to be greater than 40 km/h.

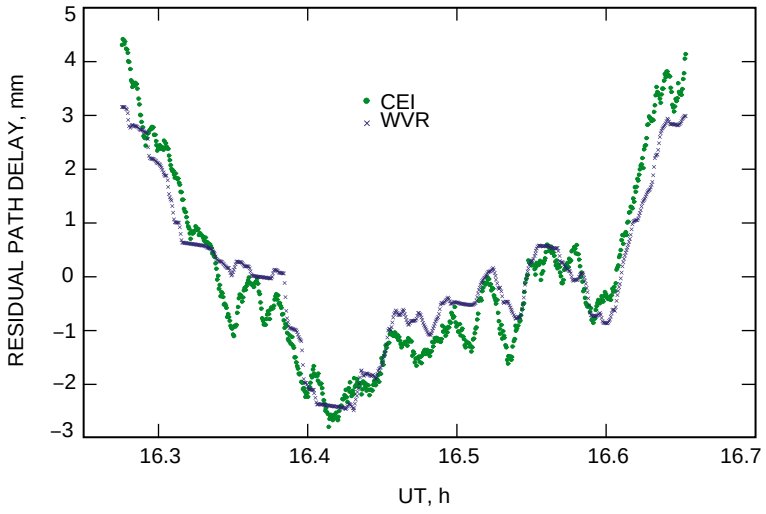

Fig. 3. The site-differenced, zenith-mapped residual-delay data from the CEI and WVR for scan 3 on DOY 240, 1999.

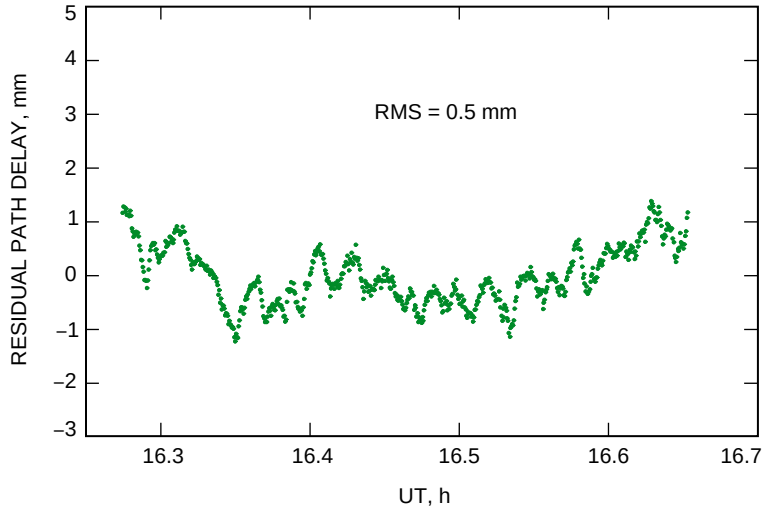

Fig. 4. The residual delay of the CEI data, scan 3 on DOY 240, 1999, after WVR corrections were applied.

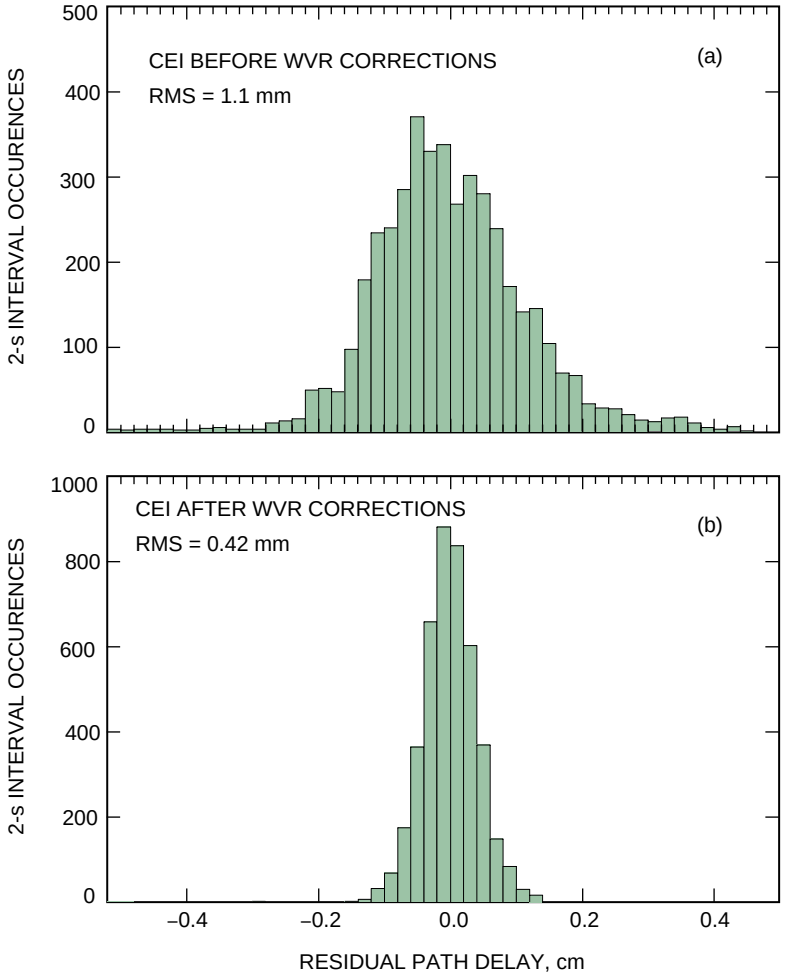

Fig. 5. Histograms of the residuals from all scans on DOY 240, 1999: (a) residual CEI path delay (rms = 1.1 mm) and (b) CEI data after WVR correction (rms = 0.42 mm).

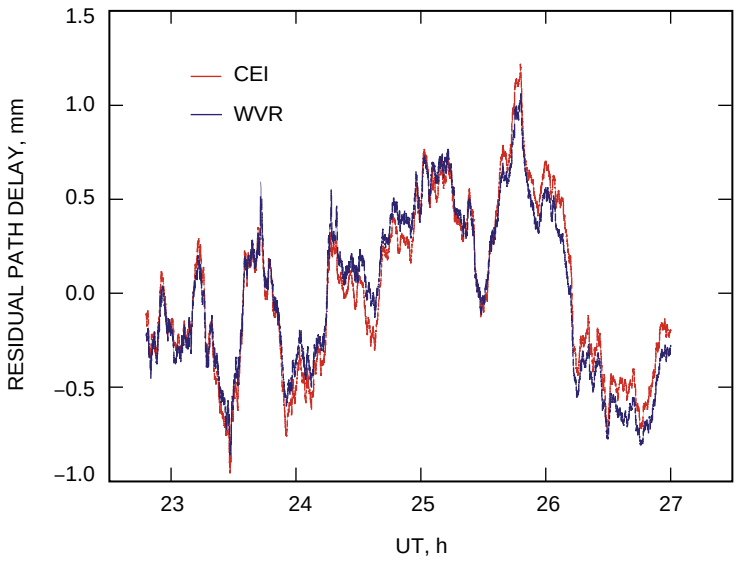

Fig. 6. The residual delay measured by the CEI and WVR for a long scan on DOY 138, 2000. The data are site-differenced, mapped to zenith, and have linear trends removed.

Figure 7 plots the Allan standard deviation (ASD) of the site-differenced delays as a function of the sampling time for DOY 138, 2000. The CEI data and WVR data have ASD values that track one another very closely over almost the entire range of sampling times. After the WVR data are used to calibrate the CEI data, the ASD decreases by a factor of 6 at time intervals greater than 1000 s. The calibrated CEI data show improvement for all sampling times down to ∼15 s, below which the 50-m WVR–DSN offset precludes useful calibration.

The solid black plot in Fig. 7 represent the Cassini GWE ASD requirement. For sampling times above 2000 s, we meet the science objectives. Below sampling times of 1000 s, we are 2 to 3 times higher than the requirements. However, this was not unexpected. Early in the design phase the cost performance trade-off studies estimated that the calibration accuracy on time scales less than 1000 s would be limited by the 50-m beam offset. This was deemed acceptable since most of the interesting gravitational wave science in the GWE is at time scales >1000 s.

III. Conclusion

We have described an atmospheric media calibration system that was shown to calibrate out the atmospheric delay fluctuations down to an Allan standard deviation level of 2×10^{-15} for sampling times greater than 1000 s. This system meets the GWE requirements for time scales greater than 2000 s. Calibration of the CEI data reduced the measured delay residuals by a factor of ∼4.

The CEI residual delay error, as illustrated in Fig. 7, is composed of the quadrature sum of the CEI errors and the WVR errors. Hence, Fig. 7 really is an upper estimate of the WVR residual delay errors. To improve upon our assessment of the WVR performance, the error budget of each measurement technique must be independently examined in greater detail. Work is now under way to critically reevaluate the WVR error budget (precision, stability, beam size, beam offset, beam mismatch, and retrieval accuracy) and the CEI error budget (electronic stability, instrumental-delay mismodeling, and baseline accuracy).

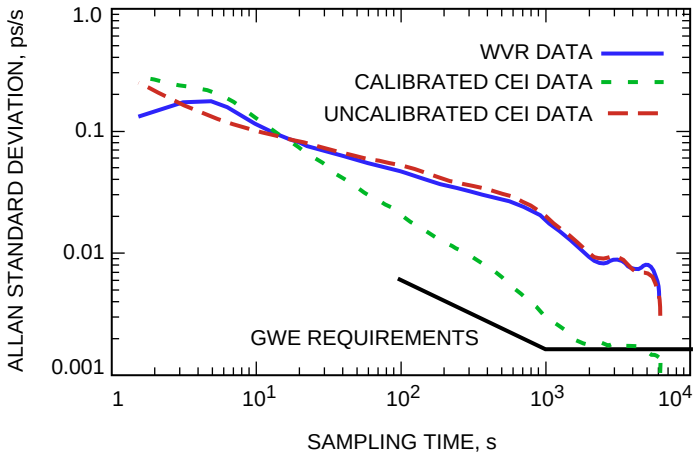

Fig. 7. The Allan standard deviation plotted as a function of sampling time for the long scan of DOY 138, 2000, showing the CEI residual data, the WVR residual data, the CEI data after WVR corrections, and the requirements for the Cassini GWE.

Acknowledgments

We would like to thank Larry Teitelbaum for helpful discussions on data analysis and John Eric Clark, Charles Snedeker, Lyle Skjerve, Leroy Tanida, the staff of DSS 13, and the operations crews at the Goldstone Signal Processing Center for the invaluable assistance provided during these operations.

References

[1] J. W. Armstrong and R. A. Sramek, "Observations of Tropospheric Phase Scintillations at 5 GHz on Vertical Paths," *Radio Science*, vol. 17, pp. 1579–1586, November 1982.

[2] M. Tinto and J. W. Armstrong "Spacecraft Doppler Tracking as a Narrow-Band Detector of Gravitational Radiation," *Phys. Rev. D*, vol. 58, article 042002, 1998.

[3] J. W. Armstrong, B. Bertotti, F. B. Estabrook, L. Iess, and H. D. Wahlquist, "The Galileo/Mars Observer/Ulysses Coincidence Experiment," *Proc. of the Second Edoardo Amaldi Conf. on Gravitational Waves*, E. Coccia, G. Pizzella, and G. Veneziano, eds., Edoardo Amaldi Foundation Series, vol. 4, World Scientific, 1998.

[4] S. J. Keihm, "Water Vapor Radiometer Measurements of the Tropospheric Delay Fluctuations at Goldstone Over a Full Year," *The Telecommunications and Data Acquisition Progress Report 42-122, April–June 1995*, Jet Propulsion Laboratory, Pasadena, California, pp. 1–11, August 15, 1995.
http://tmo.jpl.nasa.gov/tmo/progress_report/42-122/122J.pdf

[5] A. B. Tanner, "Development of a High-Stability Water Vapor Radiometer," *Radio Sci.*, vol. 33, pp. 449–462, March 1998.

[6] G. M. Resch, D. E. Hogg, and P. J. Napier, "Radiometric Correction of Atmospheric Path Length Fluctuations in Interferometric Experiments," *Radio Sci.*, vol. 19, pp. 411–422, January 1984.

[7] L. P. Teitelbaum, R. P. Linfield, G. M. Resch, S. J. Keihm, and M. J. Mahoney, "A Demonstration of Precise Calibration of Tropospheric Delay Fluctuations With Water Vapor Radiometers," *The Telecommunications and Data Acquisition Progress Report 42-126, April–June 1996*, Jet Propulsion Laboratory, Pasadena, California, pp. 1–8, August 15, 1996.
http://tmo.jpl.nasa.gov/tmo/progress_report/42-126/126H.pdf

[8] G. M. Resch, "Inversion Algorithms for Water Vapor Radiometers Operating at 20.7 and 31.4 GHz," *The Telecommunications and Data Acquisition Progress Report 42-76, October–December 1983*, Jet Propulsion Laboratory, Pasadena, California, pp. 12–26, February 15, 1984.
http://tmo.jpl.nasa.gov/tmo/progress_report/42-76/176B.PDF

[9] S. J. Keihm and K. A. Marsh, "Advanced Algorithm and System Development for Cassini Radio Science Tropospheric Calibration," *The Telecommunications and Data Acquisition Progress Report 42-127, July–September 1996*, Jet Propulsion Laboratory, Pasadena, California, pp. 1–20, November 15, 1996.
http://tmo.jpl.nasa.gov/tmo/progress_report/42-127/127A.pdf

[10] D. W. Allan, "Statistics of Atomic Frequency Standards," *Proc. IEEE*, vol. 54, no. 2, pp. 221–230, February 1966.

[11] S. Lowe, *Theory of Post-Block II VLBI Observable Extraction*, JPL Publication 92-7, Jet Propulsion Laboratory, Pasadena, California, July 15, 1992.

[12] R. P. Linfield and J. Z. Wilcox, "Radio Metric Errors Due to Mismatch and Offset Between a DSN Antenna Beam and the Beam of a Troposphere Calibration Instrument," *The Telecommunications and Data Acquisition Progress Report 42-114, April–June 1993*, Jet Propulsion Laboratory, Pasadena, California, pp. 1–13, August 15, 1993.
http://tmo.jpl.nasa.gov/tmo/progress_report/42-114/114A.pdf

[13] G. Elgered, "Tropospheric Radio Path Delay from Ground-Based Microwave Radiometry," in *Atmospheric Remote Sensing by Microwave Radiometry*, Chapter 5, M. Janssen, ed., New York: John Wiley, 1993.